Noise Induced Limit Cycles of the Bonhoeffer-Van der Pol Model of Neural Pulses

Herbert Treutlein and Klaus Schulten

Physik-Department, Technische Universität München, 8046 Garching, Federal Republic of Germany

Biophysical Chemistry / Computer Experiments / Nerve Excitation / Non-linear Phenomena / Stochastic Processes

The effect of additive noise on the Bonhoeffer-van der Pol (BvP) model is studied. For this purpose we developed a numerical algorithm to solve the pertinent 2-dim. Fokker-Planck equation. The results demonstrate that the global behaviour of the system is determined by certain lines toward which the distribution function is attracted. These lines are also the seeds for the limit cycle in the deterministic system. The noisy BvP model exhibits a limit cycle (oscillations) even when the deterministic system does not. This behaviour may explain the firing pattern of neurons.

1. Introduction

The dynamics of the voltage and the current across neural membrans which exhibits a threshold behavior and which produces the propagation of voltage pulses is one of the best known examples of non-linear behavior. In fact, non-linear rate equations can describe very well the electrical activity of certain nerve cells, the giant axons of squid, as had been shown in the celebrated work of Hodgkin and Huxley [1]. These authors established a set of 4-dimensional non-linear differential equations, the socalled Hodgkin-Huxley equations, which account rather well for the shape and the threshold behavior of nerve pulses.

After the inception of the theoretical analysis of neural activity by Hodgkin and Huxley several attempts had been made to extent the Hodgkin-Huxley equations. It has been investigated also in how far simpler dynamical models may describe the behavior of neural pulses as well. One such model originates from the work of van der Pol [2] and Bonhoeffer [3–6]. Actually, Bonhoeffer had attempted to mathematically model neural pulses independently of the work of Hodgkin and Huxley. Extending the describtion of the van der Pol oscillator he suggested the following two equations [3–6]

$$\partial_t x_1 = c(x_1 + x_2 - \tfrac{1}{3}x_1^3 + z) = F_1(x) \tag{1a}$$

$$\partial_t x_2 = -(x_1 + bx_2 - a)/c = F_2(x) \tag{1b}$$

where a, b, c, z are external parameters. It had been later shown by Fitzhugh [7] that the 4-dimensional dynamics of the Hodgkin-Huxley equations can be projected without much loss of information onto a 2-dimensional manifold and that the ensuing dynamics are reproduced by the Bonhoeffer-van der Pol equations above. In this description the variable x_1 represents approximately the voltage across the neural membrane. The description of nerve cell activity by the Bonhoeffer-van der Pol model is simpler than that by the Hodgkin-Huxley equation, mainly because of the smaller number of independent dynamic variables. In applying Eq. (1) we will adopt the following parameter values

$$a = 0.7, \quad b = 0.8, \quad c = 3.0\,. \tag{2}$$

The parameter z corresponds to the membrane current. This parameter controls the qualitative behaviour of the solution of Eq. (1) as will be discussed in section 2.

The firing pattern of neural pulses often show the following features: the shapes of individal pulses are nearly identical and frequency independent; the firing frequency can vary over a broad range; the time period between pulses shows a stochastic scatter. This behaviour cannot be understood solely on the basis of a deterministic non-linear dynamic process, e.g. the Bonhoeffer-van der Pol model, but rather requires a stochastic process as well. The source of the latter process should be the fluctuations which are always detected when neural membran conductivity is observed [8].

In the following paper we will study the effect of noise on the Bonhoeffer-van der Pol model. We will demonstrate that the noise level can be employed to tune the firing frequency of Hodgkin-Huxley type neurons. For this purpose we have considered the Fokker-Planck equation corresponding to the stochastic Bonhoeffer-van der Pol model. This equation

Ber. Bunsenges. Phys. Chem. *89*, 710–718 (1985)
0005–9021/85/0606–0710 $ 02.50/0

has been solved by a new Monte Carlo algorithm. We demonstrate that the ensuing distribution functions represent the global characteristics of the underlying force field: lines which attract nearby trajectories prove to be the regions of phase space where the distributions concentrate their amplitude. Since there are two such lines the distributions are bimodal representing repeated fluctuations between these two lines. Even in cases that the deterministic Bonhoeffer-van der Pol model does not show limit cycle behaviour we observed a stochastic limit cycle. This cycle will be identified with the firing of neural pulses.

The paper presented here is a shortened version of a more detailed publication [9].

2. Linear Stability Analysis of the Bonhoeffer-van der Pol Model

The qualitative behaviour of the solution of (1) can be examined by an analysis of the dynamics in a small neighbourhood of the stationary points (For a reference to linear stability analysis see for example Ref. [10]). The stationary points of (1) are determined through the two equations $F_1 = F_2 = 0$, i.e. through

$$x_2 = \tfrac{1}{3}x_1^3 - x_1 - z \tag{3a}$$

$$x_2 = (a - x_1)/b. \tag{3b}$$

For the parameters (2) there exists exactly one stationary point x_s the first component of which satisfies

$$z = \tfrac{1}{3}x_{s1}^3 - x_{s1}(1 - \tfrac{1}{b}) - a/b. \tag{4}$$

The Jacobian of F which determines the dynamics in linear approximation near x_s is

$$DF = \begin{pmatrix} c(1 - x_{s1}^2) & c \\ -1/c & -b/c \end{pmatrix}. \tag{5}$$

The eigenvalues of DF

$$\lambda_{1,2} = (1/2)\{c(1 - x_{s1}^2) - b/c \pm [(b/c + c(1 - x_{s1}^2))^2 - 4]^{1/2}\} \tag{6}$$

determine the stability of the system near the stationary points. For the parameters (2) and in the z-range of physiological significance $-0.6 \leq z \leq 0.2$ the eigenvalues $\lambda_{1,2}$ are complex. One determines that for $z > -0.3465$ the real parts are negative, i.e. the system has a stable focus at x_s. At $z \approx -0.3465$ the real part of $\lambda_{1,2}$ vanishes and the system undergoes a Hopt bifurkation [10, 11]. At lower values of z one expects that a stable limit cycle exists. This can be shown, in fact, for large c and positive b (Ref. [9]).

In order to demonstrate the dynamics resulting from the Bonhoeffer-van der Pol equations we present in Fig. 1a, b some sample trajectories. The trajectories in Fig. 1a correspond to the choice $z = 0$, i.e. a case that a stable focus exists which all trajectories reach asymptotically. The trajectories in Fig. 1b correspond to the choice $z = -0.4$, i.e. a situation in which a stable limit cycle is expected. All trajectories are found to converge to this limit cycle.

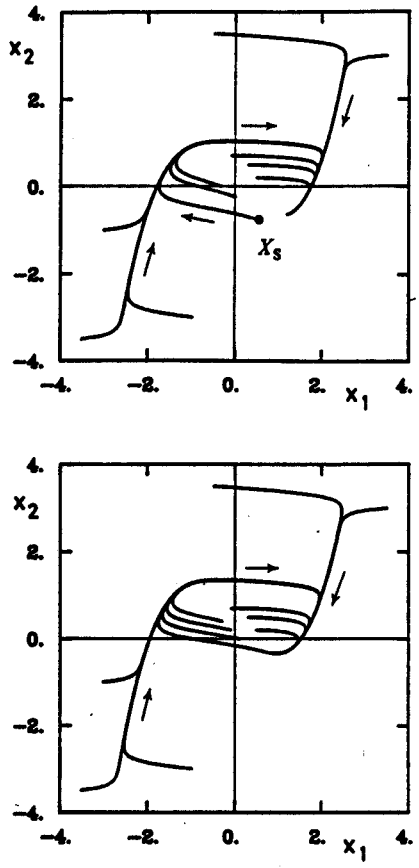

Fig. 1
Sample trajectories of the deterministic Bonhoeffer-van der Pol model as described by Eqs. (1, 2); (a) for $z = 0$, i.e. a case in which the model does not show limit cycle behavior and all trajectories end in a stable focus; (b) for $z = -0.4$, i.e. a case in which the model shows limit cycle behaviour

The following conclusions regarding the behaviour of neural pulses can be drawn from the above analysis: The variable x_1 in Fig. 1a, b represents the membrane voltage. For small membrane currents z ($-0.3465 < z < 0.2$), the situation shown in Fig. 1a, a perturbation of the voltage to lower x_1 values either results in a direct restoration of the stationary voltage or, for larger perturbations, results in a single neural pulse comprising an initial further decrease of x_1. This behaviour reflects the well-known threshold behaviour of nerve pulse generation. One would like to identify mathematically the threshold line which seperates the region of direct return and of return by single pulse generation.

For larger membrane currents ($-0.6 < z < -0.3465$), the situation shown in Fig. 1b, all conditions result in a continuous train of pulses. One may consider that this behaviour can explain the pulse trains which code the signal of single nerve fibers in neural tissue. However, there is one difficulty. The period of the limit cycle is rather invariable. Assuming that z is the variable which a nerve cell employs to tune its firing frequency such cell could only switch be-

tween a single pulse behaviour, i.e. zero frequency, and a limit cycle behaviour, i.e. a high frequency.

3. Global Analysis of the Bonhoeffer-van der Pol Model

In view of the similarity of the Bonhoeffer-van der Pol trajectories for $z=0$ and $z=-0.4$ in Fig. 1a, b it seems rather surprising that the dynamics of the two cases are so different: an asymptotic stationary state for $z=0$ and an asymptotic limit cycle for $z=-0.4$. The results below will show that the addition of noise to the Bonhoeffer-van der Pol dynamics makes the difference between the two cases disappear. We will find that the stochastic dynamics depend mainly on the global characteristics of the force field rather than on the local behaviour around the stationary points.

In order to study the global characteristics of the Bonhoeffer-van der Pol model we pose the question in which respect the force fields represented by the trajectories in Fig. 1a, b show a close comparision. The main features found in both cases are two lines on the left and right part of the x_1, x_2-phase space to which the trajectories appear to be attracted. Another feature is a line in the center of the phase space of Fig. 1a, b near which the trajectories appear to separate towards the positive and the negative x_1-axis. For the case $z=0$ this line characterizes the threshold behaviour of the Bonhoeffer-van der Pol model.

The lines we seek to describe will be called *local attractors* and *local separatrices* [9]. One main result of this paper is a demonstration of the importance of these lines, in particular for stochastic systems, a demonstration which is to be contrasted to the fact that these lines have not been given any attention since a long time. The lines are not identical to attractors or separatrices.

The *local attractors* and *local separatrices* are defined through the isoclines of the force field $\boldsymbol{F}(x)$. The isocline coding for the slope m is determined through

$$m = F_2(x_1, x_2)/F_1(x_1, x_2) . \tag{7}$$

Solving this equation for x_2 yields

$$x_2 = I(m, x_1) \tag{8}$$

which identifies all points in phase space where trajectories assume the slope m. The *local attractors* and *local separatrices* are determined through the condition that an isocline is locally tangential to a trajectory. This implies necessarily that the slope of the isocline is

$$\partial_1 I(m, x_1) = m . \tag{9}$$

This condition implies that nearby trajectories either converge to this trajectory or diverge from it. In order to solve Eq. (9) for m we employ the implicit function theorem which provides

$$m^2 \partial_2 F_1 + m(\partial_1 F_1 - \partial_2 F_2) - \partial_1 F_2 = 0 . \tag{10}$$

There exist either two real solutions

$$m = M_{1,2}(x_1, x_2) \tag{11}$$

or there does not exist any real solution. In the first case *local attractors* and *local separatrices* may exist and are determined as the pairs of coordinates which solve (11), (7). Since in the case of the Bonhoeffer-van der Pol model $M_{1,2}$ depends solely on x_1 the solution of (11), (7) are the pairs (x_1, x_2) with

$$x_2 = I[M_{1,2}(x_1), x_1] . \tag{12}$$

In order that this curve does indeed correspond to *local attractors* or *local separatrices*, i.e. is also a trajectory of (1), (12) has to satisfy the *consistency condition* [12]

$$m = \mathrm{d}_1 I[M_i(x_1), x_1] . \tag{13}$$

With (9) follows that the *consistency condition* requires

$$\partial_M I \, \partial_1 M \approx 0 . \tag{14}$$

We will find that this condition can hold only approximately. This qualification does not render our analysis worthless as is demonstrated rather dramatically in Fig. 2a, b (see also Ref. [9]).

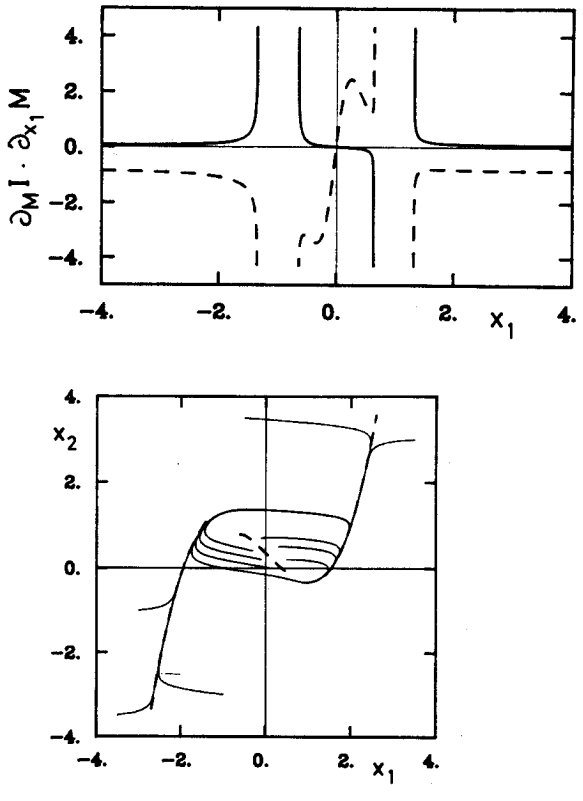

Fig. 2
(a) Test of the consistency condition $\partial_M I \, \partial_1 M = 0$ to determine which solution of (10) qualifies as an invariant line; the figure shows that one of the solutions in each solution interval approximately satisfies the consistency condition ($z=-0.4$). (b) Demonstration that the proper solutions of (14) behave as invariant lines, i.e. locally either attract or repel neighbouring trajectories ($z=-0.4$)

The force field of the Bonhoeffer-van der Pol model yields three intervals on the x_1-axis in which (10) has real solutions. Fig. 2a presents $\partial_M I\, \partial_1 M$ to test the consistency condition (14). One observes that one of the solutions approximately satisfies the condition except near the end of the solution intervals. Fig. 2b presents the lines which approximately satisfy (14). The trajectories included in this figure show clearly that these lines do indeed identify those characteristic regions of the phase space where trajectories are either syphoned together or diverge apart.

The *local attractors* shed also some light on the way the Bonhoeffer-van der Pol model yields a limit cycle. The trajectories in Fig. 1b indicate that the limit cycle does not attract nearby trajectories along its whole length. Comparision with Fig. 2b reveals that only those sections of the limit cycle which coincide with *local attractors* syphon-in trajectories. In fact, the trajectories near the remaining sections of the limit cycle may actually diverge from the limit cycle. A limit cycle can still result if the *local attractor* sections overall achieve a stronger attraction of trajectories than the remaining sections repel neighbouring trajectories. One may hence consider the *local attractors* to provide the seed for the limit cycle.

In Ref. [12] it has been shown that the *local attractors* and *local separatrices* as defined through (11), (7) are identical to those set of points where the trajectories have zero curvature. This characterization indicates that the lines described above can only be *local attractors* or *local separatrices*, i.e. trajectories of (1), if they are nearly linear. Hence the consistency condition (13) needs to be employed. We are currently further developing the calculus presented here to cover also situations where local attractors and separatrices are not nearly linear [12].

4. Stochastic Bonhoeffer-van der Pol Dynamics/Theory

In order to model stochastic effects accompanying the dynamics of neural pulse generation we envoke a noise term in the Bonhoeffer-van der Pol equations. For a first exploration of the ensuing stochastic dynamics it should suffice to choose the simplest realization of noise, namely additive noise which is isotropic in the x_1- and x_2-directions. The Bonhoeffer-van der Pol Eq. (1) are thereby replaced by the stochastic differential equation

$$\partial_t x_1 = F_1(x_1, x_2) + \sigma\, \mathrm{d}W_1(t)/\mathrm{d}t \tag{15a}$$

$$\partial_t x_2 = F_2(x_1, x_2) + \sigma\, \mathrm{d}W_2(t)/\mathrm{d}t \tag{15b}$$

where $F_i(\boldsymbol{x})$ are defined as in Eq. (1). This equation differs from the Bonhoeffer-van der Pol equation through the additive noise terms $\sigma\, \mathrm{d}W_i(t)$. $\mathrm{d}W_i(t)$ represents normalized white noise [$\mathrm{d}W_i(t)\, \mathrm{d}W_j(t) = \delta_{ij}\mathrm{d}t$] and σ the amplitude of the noise. In order to integrate the stochastic differential equation one has to adopt a specific set of rules (interpretation) to carry out integrals involving the noise term, e.g. the Ito calculus, the Stratonovitch calculus or an intermediate calculus. Since we consider in the following solely additive noise, in which case the amplitude σ is x-independent, the calculus adopted for our purpose is immaterial.

The dynamics resulting from the stochastic differential Eq. (15) can best be formulated in terms of a distribution function $p(\boldsymbol{x}, t)$ which describes the probability that an ensemble of systems obeying (15) is observed with the phase space variables $\boldsymbol{x}$ at time t. This distribution function obeys the following Fokker-Planck equation associated with (2)

$$\partial_t p(\boldsymbol{x}, t) = D\,[\partial_1^2 + \partial_2^2 - \beta \Sigma_i \partial_i F_i(\boldsymbol{x})]\, p(\boldsymbol{x}, t) \tag{16}$$

where

$$D = \sigma^2/2 \tag{17a}$$

$$\beta = 1/D \tag{17b}$$

are parameters which are commonly introduced to describe stochastic systems. In statistical mechanical applications D corresponds to the diffusion coefficient and β to the inverse temperature. This correspondence implies

$$\begin{aligned} &\text{large}\,\beta \leftrightarrow \text{weak noise} \\ &\text{small}\,\beta \leftrightarrow \text{strong noise}. \end{aligned} \tag{18}$$

The solution of the 2-dimensional Fokker-Planck Eq. (16) is a non-trivial task. To obtain the time-dependent distribution and the stationary distribution we adopted a Monte Carlo algorithm. This algorithm is a generalization of the Brownian dynamics algorithm developed in [13, 14] and has been presented and tested in Ref. [9].

It has been found [9] (see also below) that the stochastic Bonhoeffer-van der Pol model for any initial condition reaches quickly a stationary state. The corresponding stationary distribution can be determined by means of an ensemble average, i.e. simulating a large number of trajectories for a long time and monitoring the ensuing endpoint distribution. However, the stationary distribution is obtained faster by envoking a time average. This can be done by a simulation of a *single* trajectory over a long time recording the frequency with which the endpoints $\boldsymbol{x}_j$, $j = 0, 1, 2, \ldots$ fall into a volume element Δ of the phase space, e.g. around the point $\boldsymbol{x}$. This frequency identifies then the stationary distribution $p(\boldsymbol{x}, t \to \infty)\Delta$.

Our investigations in Ref. [9] have yielded the following approximate description of the stationary distribution function with stochastic limit cycle behaviour. The distribution near the limit cycle is affected by two stochastic processes, namely normal and tangential to the limit cycle, which are often approximately independent. For strong noise the tangential diffusion leads to a constant distribution and, hence, does not influence the total distribution. The normal diffusion induces a distribution amplitude on the limit cycle [9]

$$p_{\mathrm{appr}}(l) = [\beta \alpha(l)]^{1/2} \tag{19}$$

where $\alpha(l)$ is the derivative of the force normal to the limit cycle at the position l on the limit cycle ($0 \le l \le L$, L length of the limit cycle). The approximation (19) holds only for $\alpha(l) > 0$.

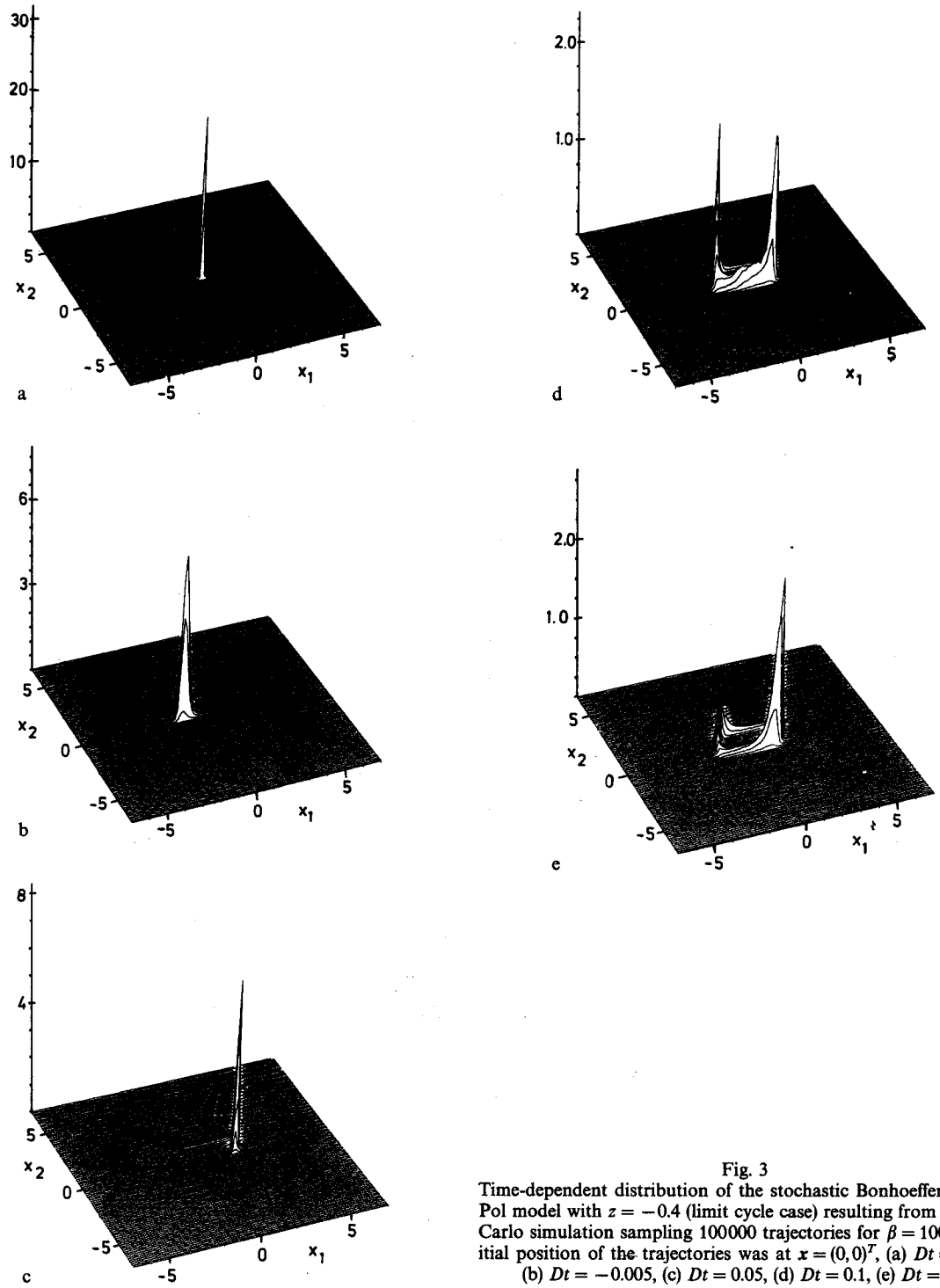

Fig. 3
Time-dependent distribution of the stochastic Bonhoeffer-van der Pol model with $z = -0.4$ (limit cycle case) resulting from a Monte Carlo simulation sampling 100000 trajectories for $\beta = 100$; the initial position of the trajectories was at $x = (0,0)^T$, (a) $Dt = 0.0005$, (b) $Dt = -0.005$, (c) $Dt = 0.05$, (d) $Dt = 0.1$, (e) $Dt = 0.3$

In case of weak noise the diffusion normal to the limit cycle does not follow adiabatically the limit cycle, i.e. the variation of $\alpha(l)$. One may, in fact, neglect the normal diffusion. The contribution of the tangential diffusion in the limit of weak noise gives the distribution

$$p_{\text{appr}}(l) = C'/F(l) \tag{20}$$

where F is the magnitude of the force on the limit cycle.

5. Stochastic Dynamics of Neural Pulses/Results

Employing the Monte Carlo method of Refs. [9, 13, 14] we have determined the time-dependent distribution for the stochastic Bonhoeffer-van der Pol model (16) at a strong noise level ($\beta = 100$) for the initial condition that the system starts at $x = (0,0)^T$ at $t = 0$. Figs. 3a–e present the 2-dimensional distribution functions at the times $Dt = 0.0005$, 0.005, 0.05, 0.1, and 0.3. Figs. 4a–e present contour maps at times $Dt = 0.01$, 0.02, 0.05, 0.1, and 0.3 which have been

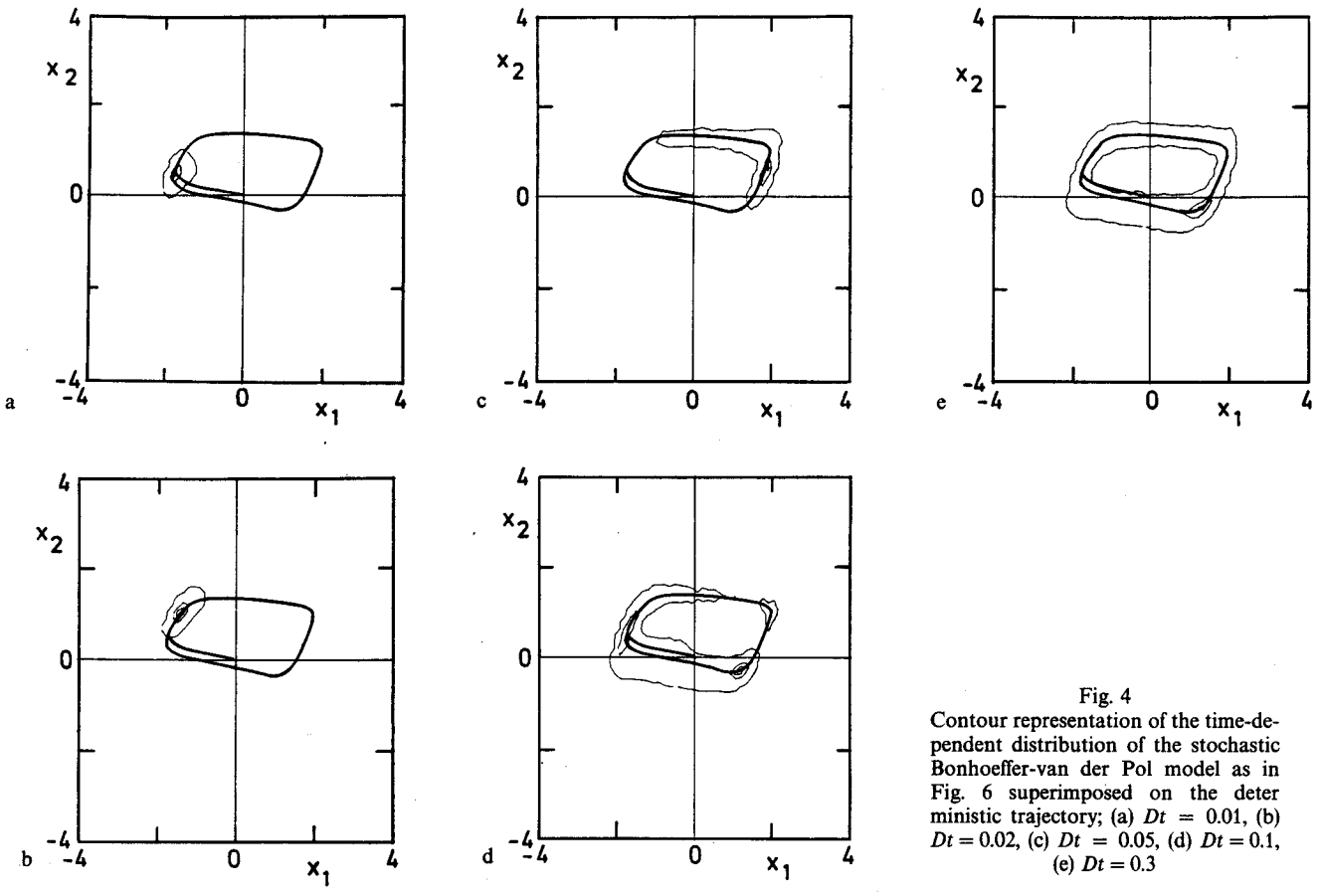

Fig. 4
Contour representation of the time-dependent distribution of the stochastic Bonhoeffer-van der Pol model as in Fig. 6 superimposed on the deter ministic trajectory; (a) $Dt = 0.01$, (b) $Dt = 0.02$, (c) $Dt = 0.05$, (d) $Dt = 0.1$, (e) $Dt = 0.3$

superimposed on the deterministic trajectory. The period DT of the limit cycle is about 0.2. Figs. 3a–c and 4a–c show the system during its approach to the limit cycle. Fig. 3a exhibits the needle like distribution peak near the origin at $t = 0.0005$ after the first time step τ. In Fig. 3b the distribution started to move rapidly towards the negative x_1-axis and broadened considerably, at least as viewed along the x_2-axis. In Fig. 4a, b the contour lines of the distribution at times $Dt = 0.01, 0.02$ show that the distribution further broadens with the peak following closely the deterministic trajectory. Figs. 3c and 4c show the system at $Dt = 0.05$, i.e. after the first quarter of the period. The distribution assumes its peak near the force minimum on the limit cycle and exhibits a long backward tail along the limit cycle. Already after half the limit cycle period, the situation shown in Figs. 3d and 4d, the distribution bifurcated into two maxima near the two minima of the limit cycle force $F(l)$. Obviously the noise advanced half of the distribution over the slow segment of the limit cycle from the right to the left side of the limit cycle. After the 1.5-fold limit cycle period, the moment exhibited by Figs. 3e and 4e, the distribution approaches its stationary form. Longer integration does not yield further changes of the distribution.

Since the stochastic Bonhoeffer-van der Pol model reaches its stationary state so rapidly this system should be sufficiently characterized by the stationary distribution which we will henceforth consider only. In this section we will study the influence of the noise level on the stationary distribution. We present for this purpose in Figs. 5a–d this distribution for noise levels corresponding to β values 200 (weak noise), 100, 10, and 1 (strong noise). The distributions are all mainly concentrated around the limit cycle. However, the distributions broaden considerably when the noise is increased as can be judged by the maximum amplitudes of the distribution which decrease from a value of 3 to a value of 0.15. For all the noise levels the distribution is bimodal with maxima along the *local attractors*. Between the *local attractors* the distribution is very broad. This underlines our remarks above on the importance of the *local attractors* for the limit cycle behaviour. They show their attraction of the stochastic trajectories in the most pronounced way for strong noise levels as shown for $\beta = 1$ in Fig. 5d. Here the distribution is not any more concentrated around the limit cycle but rather around the *local attractors* (compare with Fig. 2b). The topology of the stationary distribution is more clearly shown in Figs. 6a, b which shows for $\beta = 100$ and $\beta = 1$ the contour plots of the distributions superimposed on the deterministic limit cycle.

In order to test the calculated distributions we compare in Figs. 7a, b the amplitudes along the limit cycle for weak (a) and strong (b) noise levels with the analytical approximations (19) and (20), respectively. The comparision is satisfactory. The deviations in Fig. 7a are due to the fact that $\beta = 200$ is not yet large enough to represent the limit of weak noise where (20) holds. The deviation in Fig. 7b are in the sections of the limit cycle between the invariant lines

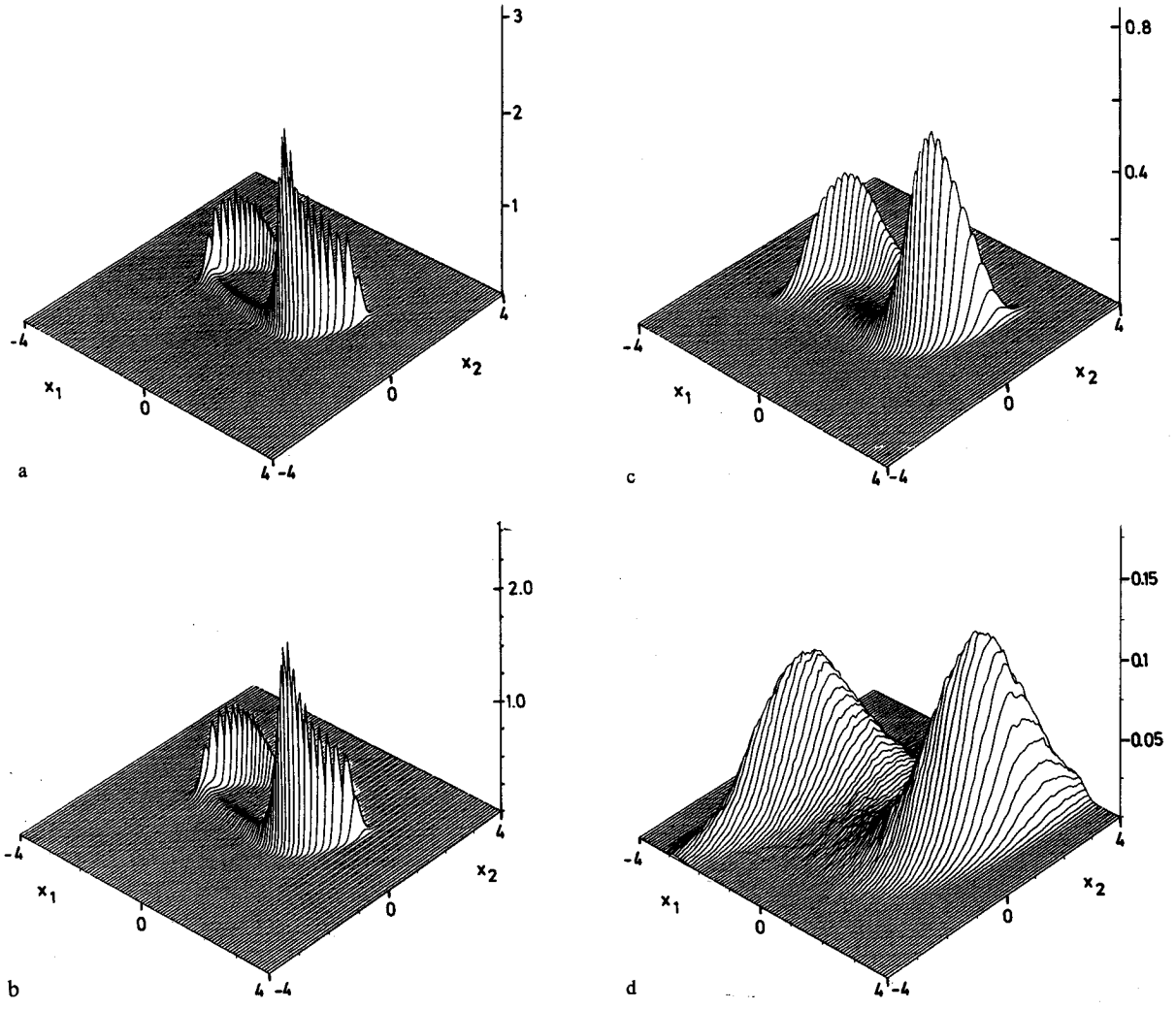

Fig. 5
Stationary distribution of the stochastic Bonhoeffer-van der Pol model with $z = -0.4$ for different noise levels; the distributions resulted from single Monte Carlo trajectories sampling about 29000000 points; (a) $\beta = 200$, (b) $\beta = 100$, (c) $\beta = 10$, (d) $\beta = 1$

where $\alpha(I) < 0$ and where the approxiamtion (19) does not hold. In these sections the distribution function does not diverge apart infinitely fast but rather exhibits a slowly decaying tail which connects the two *local attractors.*

We want to consider now the stochastic Bonhoeffer-van der Pol model in the case of zero membrane current, i.e. $z = 0$. For this z value the deterministic model does not show a limit cycle behaviour but rather approaches a stable focus. Figs. 8a, b show the stationary distribution of the stochastic system for the two noise levels $\beta = 10$ and $\beta = 100$. A comparision of the distributions of Figs. 5c and 8a which both correspond to $\beta = 10$ but to different z values, namely $z = -0.4$ and $z = 0$, respectively, shows that the stochastic system for $z = 0$ behaves almost identical to the $z = -0.4$ limit cycle system. The difference in the behaviour between the stochastic system and the deterministic system is demonstrated in Fig. 9 which presents the contour lines to Fig. 8a superimposed on a deterministic trajectory. This trajectory approaches most directly the stable focus. In contrast the stochastic system exhibits a bimodal distribution which represents repeated jumps of stochastic trajectories between the *local attractors.* Even in the case of weak noise the distribution is bimodal as seen in Fig. 8b. The interpretation of this finding is that the noise induces the Bonhoeffer-van der Pol model to move along a limit cycle in a parameter range where the deterministic system does not show limit cycle behaviour.

We finally demonstrate that neurons may vary their firing rate by means of a noise induced limit cycle behavior. Figs. 10a, b show time traces of the x_1 variable of the stochastic Bonhoeffer-van der Pol model for $z = -0.4$ (a) and $z = 0$ (b), i.e. the cases in which the deterministic system does and does not show a limit cycle. The traces of x_1 are remarkably similar to physiological recordings of single nerve cells in that the shapes of single pulses are rather invariant and a scatter in the time between pulses is observed. The recording of the system in Fig. 10b corresponds to the distribution in Fig. 8b. Every pulse corresponds to a circulation along a noise-induced limit cycle.

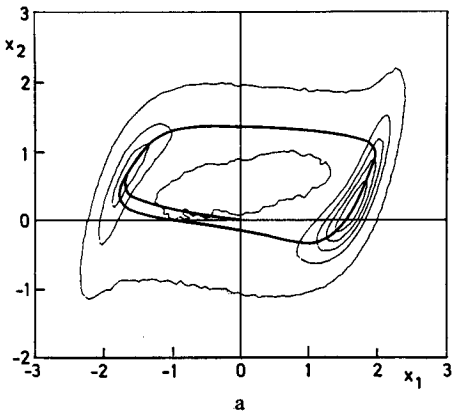

a

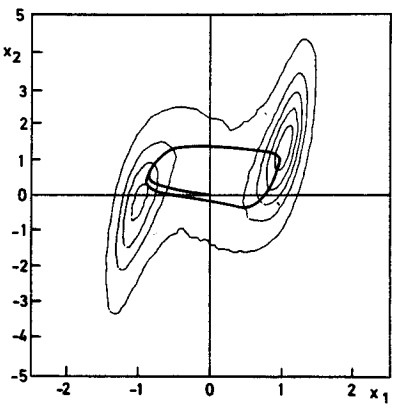

b

Fig. 6
Contour plot representation of the stationary distributions of the stochastic Bonhoeffer-van der Pol model with $z = -0.4$ resulting from single trajectories sampling about 10^6 jump points superimposed on a deterministic trajectory which illustrates the limit cycle; (a) $\beta = 100$, (b) $\beta = 1$

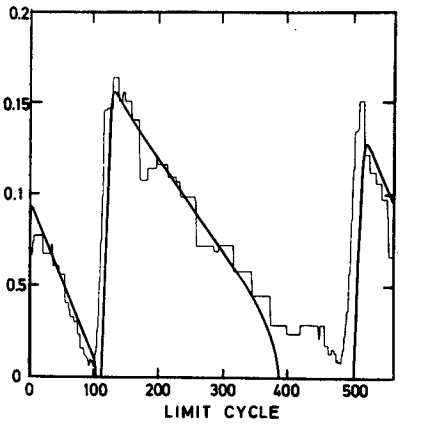

b

Fig. 7
Stationary distribution of the stochastic Bonhoeffer-van der Pol model with $z = -0.4$ along the limit cycle; the figures compare the distribution obtained by Monte Carlo simulation sampling about 10^6 jump points of a single trajectory with analytical approximations; (a) limit of weak noise ($\beta = 200$) comparing to approximation (20); (b) limit of strong noise ($\beta = 1$) comparing to approximation (19)

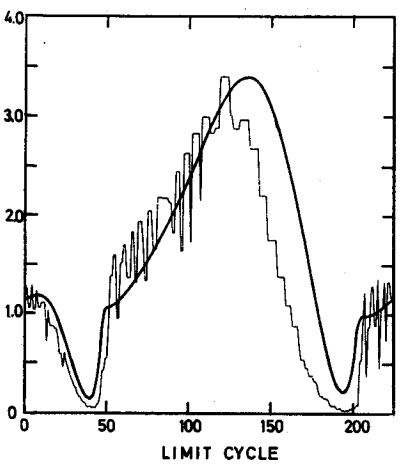

a

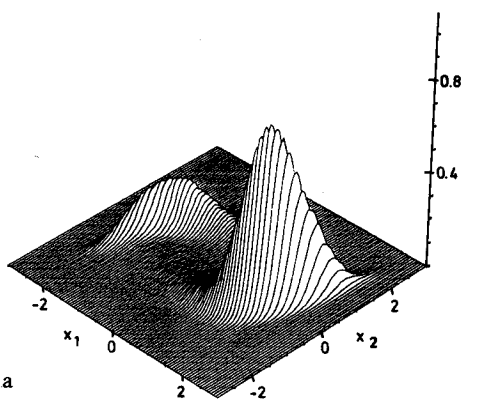

a

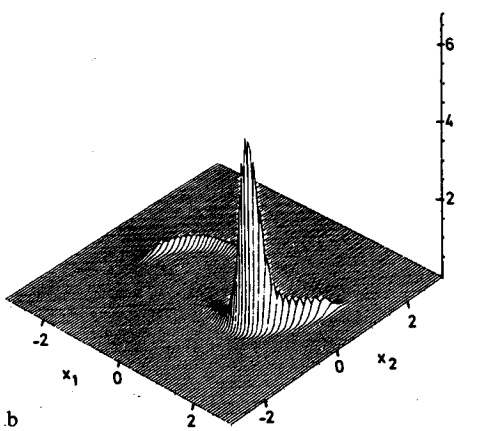

b

Fig. 8
Stationary distribution of the stochastic Bonhoeffer-van der Pol model for $z = 0$, i.e. the case that no deterministic limit cycle exists; the distribution results from a Monte Carlo trajectory sampling about 29000000 jump points; (a) $\beta = 10$, (b) $\beta = 100$

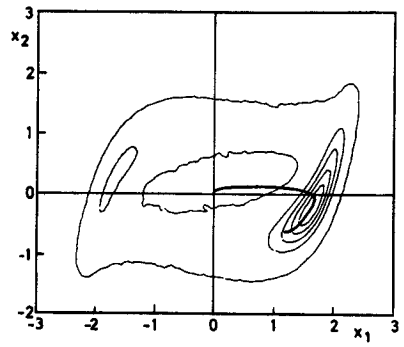

Fig. 9
Contour plot representation of the distribution in Fig. 8a superimposed on a deterministic trajectory

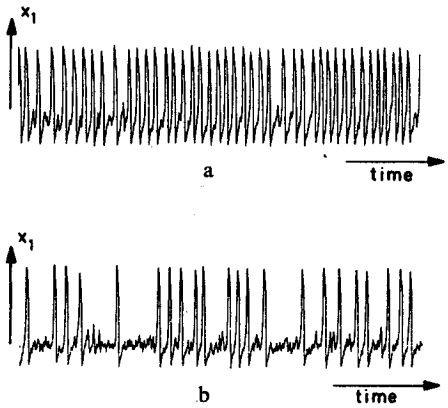

Fig. 10
Trace of the x_1 variable of a Monte Carlo trajectory for the stochastic Bonhoeffer-van der Pol model with $\beta = 100$ representing the electrical membrane potential of a neuron; (a) $z = -0.4$ (limit cycle situation), (b) $z = 0$ (no limit cycle)

The question how the frequency of pulses varies when the system parameters are changed is addressed in the two diagrams of Figs. 11a, b. Fig. 11a shows for the case $z = 0$ how the mean period between pulses depends on the noise level as measured by β. Variation of β from $\beta = 0$ to $\beta = 600$ alters the mean period between pulses by about 20 percent, i.e. not considerably. A larger variation can be induced by means of the membrane current z. Altering z from about -0.8 to about 0.2 induces a 6-fold increase of the mean time between pulses. Further variation of z increases the time even further such that the pulse frequency can virtually be varied continuously from zero to a high value. On the basis of this result we like to suggest that neurons in order to code the frequency of their axonic pulses may employ intrinsic electrical membrane noise or may use for that purpose the electrical signals of synapses converging on them (which most likely appear like noise).

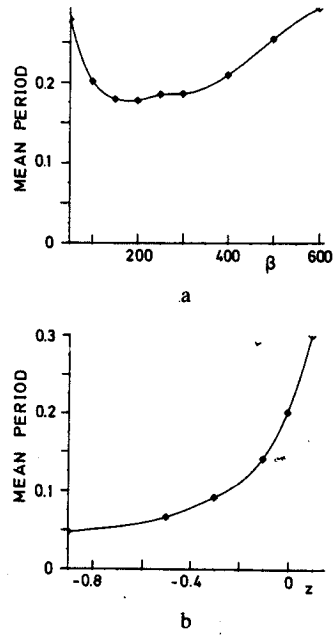

Fig. 11
Mean period between neural pulses for the stochastic Bonhoeffer-van der Pol model as described by Monte Carlo simulation; (a) dependence on the noise level for $z = 0$, (b) dependence on the current z for a constant noise level $\beta = 100$

The authors like to express their gratitude to Christoph von der Malsburg for introducing them to the subject of this article and for his patient criticism and advice. H. T. is gratefull to Mr. and Mrs. R. Treutlein for financial support which in lieu of other support made this work possible. The authors acknowledge the extensive use of the computer facilities of the Leibniz Rechenzentrum.

References

[1] A. L. Hodgkin and A. F. Huxley, J. Physiol. London *117*, 500 (1952).
[2] B. van der Pol, Philos. Mag. *2*, 978 (1926).
[3] K. F. Bonhoeffer, Z. Elektrochem. *47*, 147 (1941).
[4] K. F. Bonhoeffer, J. Gen. Physiol. *32*, 69 (1948).
[5] K. F. Bonhoeffer, Naturwissenschaften *40*, 301 (1953).
[6] K. F. Bonhoeffer and G. Langhammer, Z. Elektrochem. *52*, 67 (1948).
[7] R. Fitzhugh, Biophys. J. *1*, 445 (1961).
[8] See for example: B. Sackmann and E. Neher, Eds., Single – Channel Recordings. Plenum press, New York 1983.
[9] H. Treutlein and K. Schulten, submitted to Europ. Bioph. J.
[10] J. Guckenheim and P. Holmes, Nonlinear Oszillations, Dynamical systems, and Bifurcation of Vector Fields (Appl. Math. Sci., Vol. 42), Springer, Berlin-Heidelberg-New York 1983.
[11] J. Marsden and M. McCracken, The Hopf-Bifurcation and its Applications (Appl. Math. Sci., Vol. 19), Springer, Berlin-Heidelberg-New York 1976.
[12] W. Bauer, K. Schulten, Z. Schulten, and H. Treutlein, (in preparation).
[13] G. Lamm and K. Schulten, J. Chem. Phys. *75*, 365 (1981).
[14] G. Lamm and K. Schulten, J. Chem. Phys. *78*, 2713 (1983).

Presented at the Discussion Meeting of the Deutsche Bunsen-Gesellschaft für Physikalische Chemie "Dynamically Organized Systems" at Schloß Elmau, October 15th–17th, 1984

E 5991